Project	**IEEE 802.16 Broadband Wireless Access Working Group <http://ieee802.org/16>**	
Title	**Channel Models for Fixed Wireless Applications**	
Date Submitted	**2001-07-17**	
Source(s)	V. Erceg, Iospan Wireless Inc., USA	Voice: 408-232-7551, verceg@iospanwireless.com
	K.V. S. Hari, Stanford University, USA	Voice: 650-724-3640, hari@rascals.stanford.edu
	M.S. Smith, Nortel Networks, GB	Voice: +44-127-940-2128, mss@nortelnetworks.com
	D.S. Baum, Stanford University, USA	Voice: 650-724-3640, dsbaum@stanford.edu
	K.P. Sheikh, Sprint, USA	Voice: 913-315-9420, khurram.p.sheikh@mail.sprint.com
	C. Tappenden, Nortel Networks, CND	Voice: 613-763-9894, ctappend@nortelnetworks.com
	J.M. Costa, Nortel Networks, CND	Voice: 613-763-7574, costa@nortelnetworks.com
	C. Bushue, Sprint, USA	Voice: 913-624-3090, carl.bushue@mail.sprint.com
	A. Sarajedini, BeamReach Networks	Voice: 650-944-1294, asarajedini@beamreachnetworks.com
	R. Schwartz, BeamReach Networks	Voice: 650-988-4758, rschwartz@beamreachnetworks.com
	D. Branlund, BeamReach Networks	Voice: 650-988-4703, dbranlund@beamreachnetworks.com
	T. Kaitz, BreezeCOM	Voice: +972-3-645-6273, talk@breezecom.co.il
	D. Trinkwon	Voice: 650-245-5650, trinkwon@compuserve.com
Re:	Call for Contributions: Session #10 Topic: Traffic, Deployment, and Channel Models, dated September 15, 2000 (IEEE 802163-00/13) This responds to the second item: Channel propagation model	
Abstract	This document provides a joint submission that describes a set of channel models suitable for fixed wireless applications.	
Purpose	This is for use by the Task Group to evaluate air interface performance	
Notice	This document has been prepared to assist IEEE 802.16. It is offered as a basis for discussion and is not binding on the contributing individual(s) or organization(s). The material in this document is subject to change in form and content after further study. The contributor(s) reserve(s) the right to add, amend or withdraw material contained herein.	
Release	The contributor grants a free, irrevocable license to the IEEE to incorporate text contained in this contribution, and any modifications thereof, in the creation of an IEEE Standards publication; to copyright in the IEEE's name any IEEE Standards publication even though it may include portions of this contribution; and at the IEEE's sole discretion to permit others to reproduce in whole or in part the resulting IEEE Standards publication. The contributor also acknowledges and accepts that this contribution may be made public by IEEE 802.16.	
Patent Policy and Procedures	The contributor is familiar with the IEEE 802.16 Patent Policy and Procedures (Version 1.0) <http://ieee802.org/16/ipr/patents/policy.html>, including the statement "IEEE standards may include the known use of patent(s), including patent applications, if there is technical justification in the opinion of the standards-developing committee and provided the IEEE receives assurance from the patent holder that it will license applicants under reasonable terms and conditions for the purpose of implementing the standard." Early disclosure to the Working Group of patent information that might be relevant to the standard is essential to reduce the possibility for delays in the development process and increase the likelihood that the draft publication will be approved for publication. Please notify the Chair <mailto:r.b.marks@ieee.org> as early as possible, in written or electronic form, of any patents (granted or under application) that may cover technology that is under consideration by or has been approved by IEEE 802.16. The Chair will disclose this notification via the IEEE 802.16 <http://ieee802.org/16/ipr/patents/notices>.	

Channel Models for Fixed Wireless Applications

Background

An important requirement for assessing technology for Broadband Fixed Wireless Applications is to have an accurate description of the wireless channel. Channel models are heavily dependent upon the radio architecture. For example, in first generation systems, a super-cell or “single-stick” architecture is used where the Base Station (BTS) and the subscriber station are in Line-of-Sight (LOS) condition and the system uses a single cell with no co-channel interference. For second generation systems a scalable multi-cell architecture with Non-Line-of-Sight (NLOS) conditions becomes necessary. In this document a set of propagation models applicable to the multi-cell architecture is presented. Typically, the scenario is as follows:

- Cells are < 10 km in radius, variety of terrain and tree density types
- Under-the-eave/window or rooftop installed directional antennas (2 – 10 m) at the receiver
- 15 - 40 m BTS antennas
- High cell coverage requirement (80-90%)

The wireless channel is characterized by:

- Path loss (including shadowing)
- Multipath delay spread
- Fading characteristics
- Doppler spread
- Co-channel and adjacent channel interference

*It is to be noted that these parameters are random and only a statistical characterization is possible. Typically, the mean and variance of parameters are specified***.**

The above propagation model parameters depend upon terrain, tree density, antenna height and beamwidth, wind speed, and season (time of the year).

This submission combines and elaborates on contributions [7], [8], and [16] which were presented at the IEEE 802.16.3 meeting in Tampa, FL, on November 7, 2000.

Suburban Path Loss Model

The most widely used path loss model for signal strength prediction and simulation in macrocellular environments is the Hata-Okumura model [1,2]. This model is valid for the 500-1500 MHz frequency range, receiver distances greater than 1 km from the base station, and base station antenna heights greater than 30 m. There exists an elaboration on the Hata-Okumura model that extends the frequency range up to 2000 MHz [3]. It was found that these models are not suitable for lower base station antenna heights, and hilly or moderate-to-heavy wooded terrain. To correct for these limitations, we propose a model presented in [4]. The model covers three most common terrain categories found across the United States. However, other sub-categories and different terrain types can be found around the world.

The maximum path loss category is hilly terrain with moderate-to-heavy tree densities (Category A). The minimum path loss category is mostly flat terrain with light tree densities (Category C). Intermediate path loss condition is captured in Category B. The extensive experimental data was collected by AT&T Wireless Services across the United States in 95 existing macrocells at 1.9 GHz. For a given close-in distance d_0, the median path loss (PL in dB) is given by

$$PL = A + 10\,\gamma \log_{10}(d/d_0) + s \quad \text{for } d > d_0,$$

where $A = 20 \log_{10}(4\,\pi\, d_0 / \lambda)$ (λ being the wavelength in m), γ is the path-loss exponent with $\gamma = (a - b\, h_b + c / h_b)$ for h_b between 10 m and 80 m (h_b is the height of the base station in m), $d_0 = 100$m and a, b, c are constants dependent on the terrain category given in [4] and reproduced below.

Model parameter	Terrain Type A	Terrain Type B	Terrain Type C
A	4.6	4	3.6
B	0.0075	0.0065	0.005
C	12.6	17.1	20

The shadowing effect is represented by s, which follows lognormal distribution. The typical value of the standard deviation for s is between 8.2 and 10.6 dB, depending on the terrain/tree density type [4].

Receive Antenna Height and Frequency Correction Terms

The above path loss model is based on published literature for frequencies close to 2 GHz and for receive antenna heights close to 2 m. In order to use the model for other frequencies and for receive antenna heights between 2 m and 10 m, correction terms have to be included. The path loss model (in dB) with the correction terms would be

$$PL_{modified} = PL + \Delta PL_f + \Delta PL_h$$

where PL is the path loss given in [4], ΔPL_f (in dB) is the frequency correction term [5,6] given by

$$\Delta PL_f = 6 \log (f / 2000)$$

where f is the frequency in MHz, and ΔPL_h (in dB) is the receive antenna height correction term given by

$\Delta PL_h = - 10.8 \log (h / 2)$; for Categories A and B [7]

$\Delta PL_h = - 20 \log (h / 2)$; for Category C [1]

where h is the receive antenna height between 2 m and 10 m.

Urban (Alternative Flat Suburban) Path Loss Model

In [8], it was shown that the Cost 231 Walfish-Ikegami (W-I) model [9] matches extensive experimental data for flat suburban and urban areas with uniform building height. It has been also found that the model presented in the previous section for the Category C (flat terrain, light tree density) is in a good agreement with the Cost 231 W-I model for suburban areas, providing continuity between the two proposed models.

Figure 1. compares a number of published path loss models for suburban morphology with an empirical model based on drive tests in the Dallas-Fort Worth area [9]. The Cost 231 Walfisch-Ikegami model (see Appendix A) was used with the following parameter settings

Frequency = 1.9 GHz
Mobile Height = 2 m
Base Height = 30 m
Building spacing = 50 m
Street width = 30 m
Street orientation = 90°

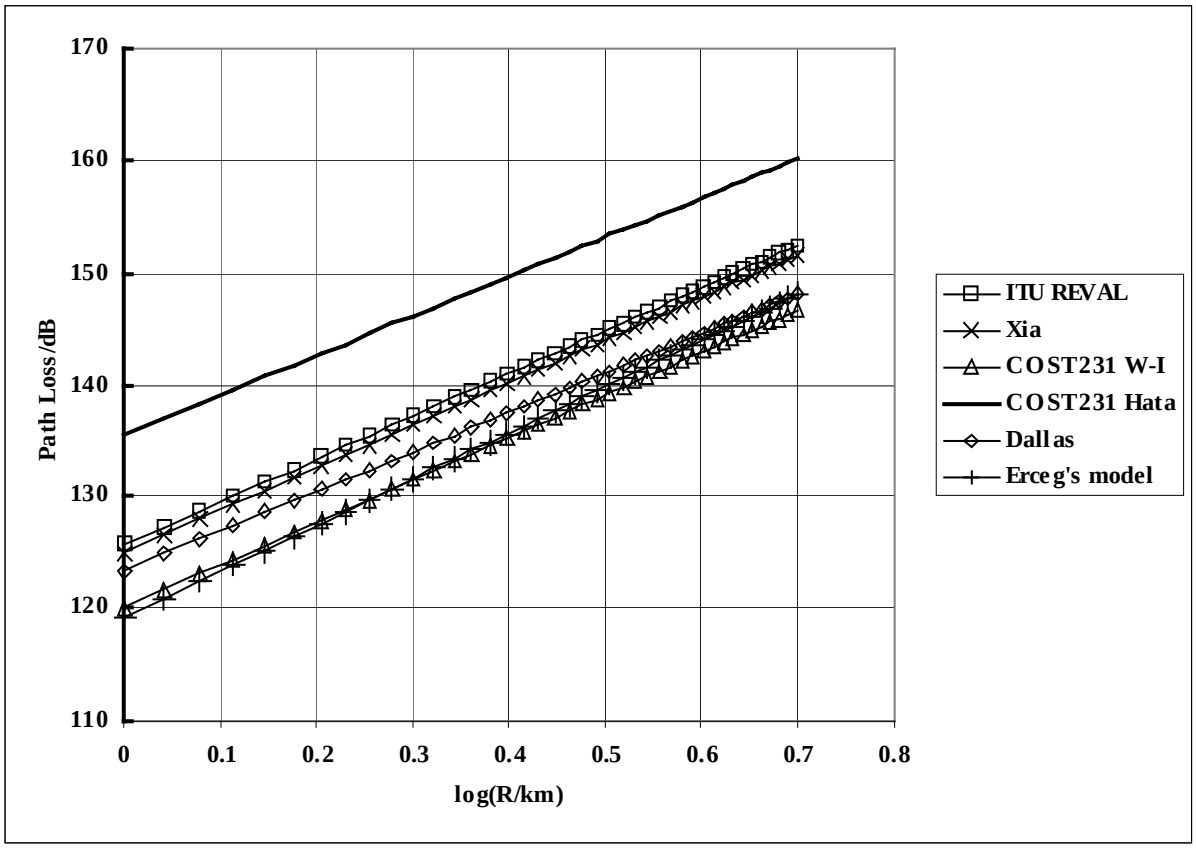

Figure 1. Comparison of suburban path loss models.

Note: COST 231 W-I, ITU Reval and Xia models all have a Hata correction term added for modeling the path loss variation with mobile height (see Appendix A).

It has also been found that the Cost 231 W-I model agrees well with measured results for urban areas, provided the appropriate building spacing and rooftop heights are used. It can therefore be used for both suburban and urban areas, and can allow for variations of these general categories between and within different countries.

Flat terrain models in conjunction with terrain diffraction modeling for hilly areas can be used in computer based propagation tools that use digital terrain databases. In [9] it was found that the weighting term for knife-edge diffraction should be set to 0.5 to minimize the lognormal standard deviation of the path loss.

Multipath Delay Profile

Due to the scattering environment, the channel has a multipath delay profile. For directive antennas, the delay profile can be represented by a spike-plus-exponential shape [10]. It is characterized by τ_{rms} (RMS delay spread of the entire delay profile) which is defined as

$$\tau^2_{rms} = \sum_j P_j \tau^2_j - (\tau_{avg})^2$$

where

$$\tau_{avg} = \sum_j P_j \tau_j ,$$

τ_j is the delay of the j th delay component of the profile and P_j is given by

P_j = (power in the j th delay component) / (total power in all components).

The delay profile has been modeled using a spike-plus-exponential shape given by

$$P(\tau) = A\,\delta(\tau) + B \sum_{i=0}^{\infty} \exp(-i\Delta\tau/\tau_0)\,\delta(\tau - i\Delta\tau),$$

where A, B and $\Delta\tau$ are experimentally determined.

RMS Delay Spread

A delay spread model was proposed in [11] based on a large body of published reports. It was found that the rms delay spread follows lognormal distribution and that the median of this distribution grows as some power of distance. The model was developed for rural, suburban, urban, and mountainous environments. The model is of the following form

$$\tau_{rms} = T_1\, d^{\varepsilon}\, y$$

where τ_{rms} is the rms delay spread, d is the distance in km, T_1 is the median value of τ_{rms} at d = 1 km, ε is an exponent that lies between 0.5-1.0, and y is a lognormal variate. The model parameters and their values can be found in Table III of [11]. However, these results are valid only for omnidirectional antennas. To account for antenna directivity, results reported in [10,12] can be used. It was shown that 32^o and 10^o directive antennas reduce the median τ_{rms} values for omnidirectional antennas by factors of 2.3 and 2.6, respectively.

Depending on the terrain, distances, antenna directivity and other factors, the rms delay spread values can span from very small values (tens of nanoseconds) to large values (microseconds).

Fading Characteristics

Fade Distribution, K-Factor

The narrow band received signal fading can be characterized by a Ricean distribution. The key parameter of this distribution is the K-factor, defined as the ratio of the “fixed” component power and the “scatter” component power. In [13], an empirical model was derived from a 1.9 GHz experimental data set collected in typical suburban environments for transmitter antenna heights of approximately 20 m. In [14], an excellent agreement with the model was reported using an independent set of experimental data collected in San Francisco Bay Area at 2.4 GHz and similar antenna heights. The narowband K-factor distribution was found to be lognormal, with the median as a simple function of season, antenna height, antenna beamwidth, and distance. The standard deviation was found to be approximately 8 dB.

The model presented in [13] is as follows

$$K = F_s\, F_h\, F_b\, K_o\, d^{\gamma}\, u$$

where

F_s is a seasonal factor, F_s =1.0 in summer (leaves); 2.5 in winter (no leaves)

F_h is the receive antenna height factor, $F_h = (h/3)^{0.46}$; (h is the receive antenna height in meters)

F_b is the beamwidth factor, $F_b = (b/17)^{-0.62}$; (b in degrees)

K_o and γ are regression coefficients, $K_o = 10$; $\gamma = -0.5$

u is a lognormal variable which has zero dB mean and a std. deviation of 8.0 dB.

Using this model, one can observe that the K-factor decreases as the distance increases and as antenna beamwidth increases. We would like to determine K-factors that meet the requirement that 90% of all locations within a cell have to be services with 99.9% reliability. The calculation of K-factors for this scenario is rather complex since it also involves path loss, delay spread, antenna correlation (if applicable), specific modem characteristics, and other parameters that influence system performance. However, we can obtain an approximate value as follows: First we select 90% of the users with the highest K-factors over the cell area. Then we obtain the approximate value by selecting the minimum K-factor within the set. For a typical deployment scenario (see later section on SUI channel models) this value of K-factor can be close or equal to 0.

Figure 2 shows fading cumulative distribution functions (CDFs) for various K factors. For example, for K = 0 dB (linear K = 1) a 30 dB fade occurs 10^{-3} of the time, very similar to a Rayleigh fading case (linear K = 0). For a K factor of 6 dB,

the probability of a 30 dB fade drops to 10^{-4}. The significance of these fade probabilities depends on the system design, for example whether diversity or retransmission (ARQ) is provided, and the quality of service (QoS) being offered.

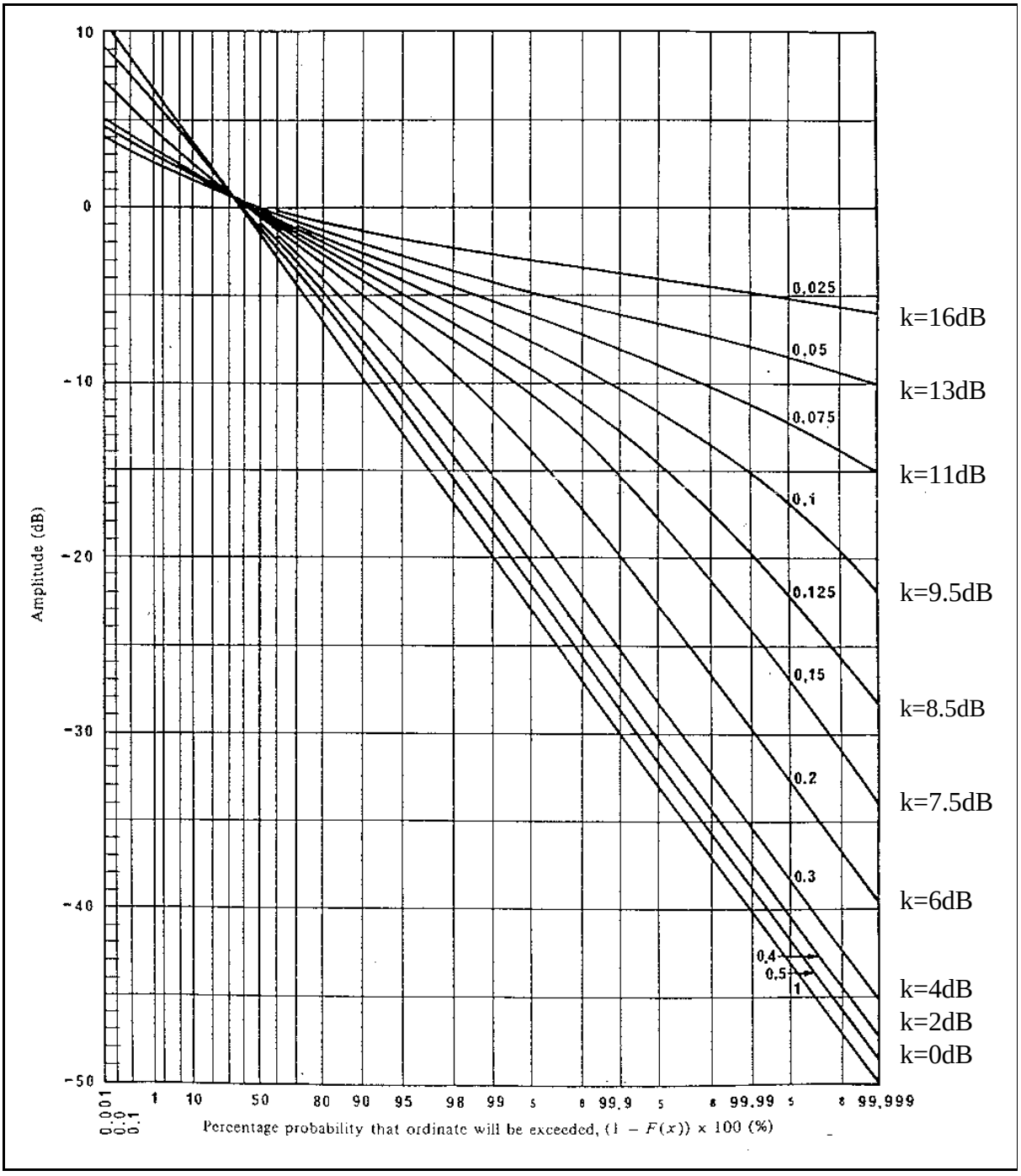

Figure 2. Ricean fading distributions.

Doppler Spectrum

Following the Ricean power spectral density (PSD) model in COST 207 [18], we define scatter and fixed Doppler spectrum components. In fixed wireless channels the Doppler PSD of the scatter (variable) component is mainly distributed around f = 0 Hz (Fig. 3a). The shape of the spectrum is therefore different than the classical Jake's spectrum for mobile channels. A rounded shape as shown in Fig. 3b can be used as a rough approximation to the Doppler PSD which has the advantage that it is readily available in most existing radio frequency (RF) channel simulators [17]. It can be approximated by:

$$S(f) = \begin{cases} 1 - 1.72 f_0^2 + 0.785 f_0^4 & f_0 \le 1 \\ 0 & f_0 > 1 \end{cases} \qquad \text{where} \quad f_0 = \frac{f}{f_m}$$

The function is parameterized by a maximum Doppler frequency f_m. Alternatively, the –3dB point can be used as a parameter, where f_{-3dB} can be related to f_m using the above equation. Measurements at 2.5 GHz center frequency show maximum f_{-3dB} values of about 2 Hz. A better approximation of fixed wireless PSD shapes are close to exponential functions [14]. Wind speed combined with foliage (trees), carrier frequency, and traffic influence the Doppler spectrum. The PSD function of the fixed component is a Dirac impulse at f = 0 Hz.

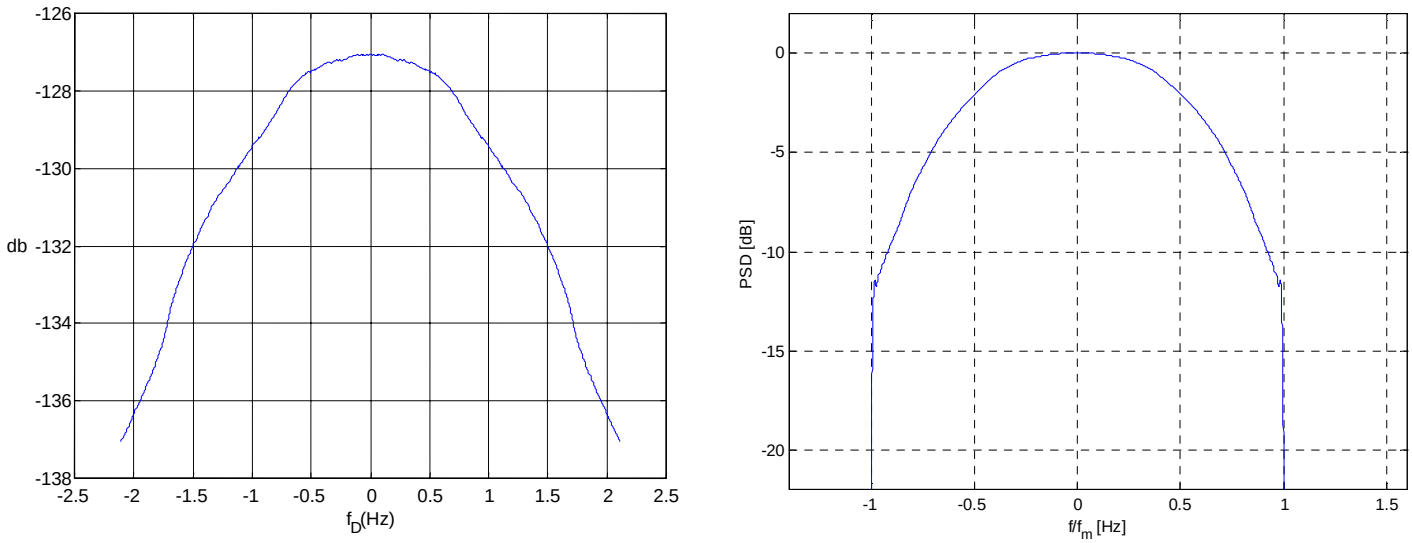

Figure 3. a) Measured Doppler spectrum at 2.5 GHz center frequency (left)
b) Rounded Doppler PSD model (right)

Spatial Characteristics, Coherence Distance

Coherence distance is the minimum distance between points in space for which the signals are mostly uncorrelated. This distance is usually grater than 0.5 wavelengths, depending on antenna beamwidth and angle of arrival distribution. At the BTS, it is common practice to use spacing of about 10 and 20 wavelengths for low-medium and high antenna heights, respectively (120^o sector antennas).

Co-Channel Interference

C/I calculations use a path loss model that accounts for median path loss and lognormal fading, but not for 'fast' temporal fading. In the example shown in Fig. 4, a particular reuse pattern has been simulated with r^2 or r^3 signal strength distance dependency, with apparently better C/I for the latter. However, for non-LOS cases, temporal fading requires us to allow for a fade margin. The value of this margin depends on the Ricean K-factor of the fading, the QoS required and the use of any fade mitigation measures in the system. Two ways of allowing for the fade margin then arise; either the C/I cdf is shifted left as shown below or the C/I required for a non-fading channel is increased by the fade margin. For example, if QPSK requires a C/I of 14 dB without fading, this becomes 24 dB with a fade margin of 10 dB.

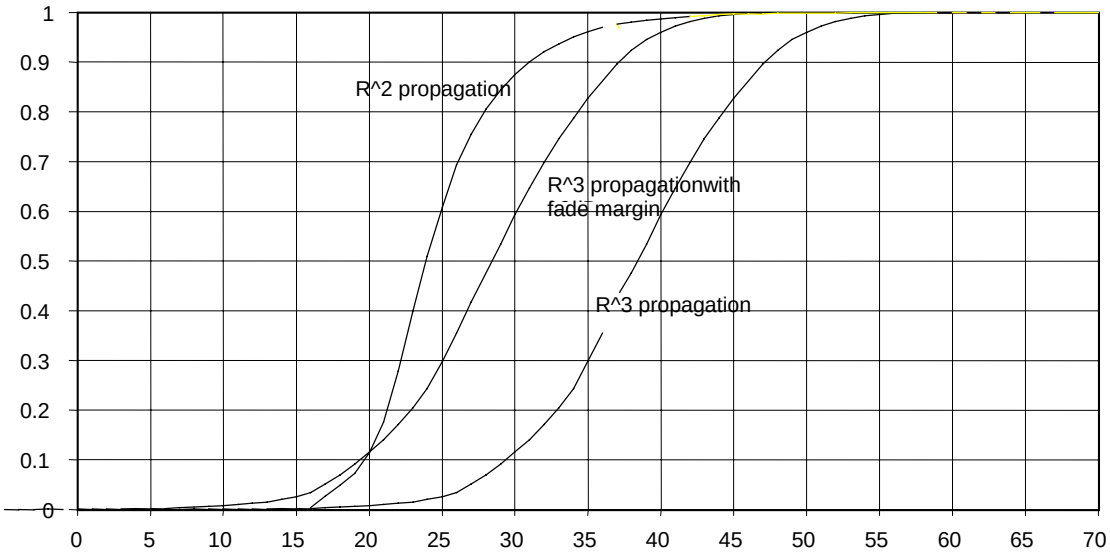

Figure 4. Effects of fade margin on C/I distributions.

Antenna Gain Reduction Factor

The use of directional antennas needs to be considered carefully. The gain due to the directivity can be reduced because of the scattering. The effective gain is less than the actual gain. This has been characterized in [15] as *Antenna Gain Reduction Factor* (GRF). This factor should be considered in the link budget of a specific receiver antenna configuration.

Denote ΔG_{BW} as the Gain Reduction Factor. This parameter is a random quantity which dB value is Gaussian distributed (truncated at 0 dB) with a mean (μ_{grf}) and standard deviation (σ_{grf}) given by

$$\mu_{grf} = - (0.53 + 0.1\, I) \ln (\beta/360) + (0.5 + 0.04\, I) (\ln (\beta/360))^2$$

$$\sigma_{grf} = - (0.93 + 0.02\, I) \ln (\beta/360),$$

β is the beamwidth in degrees

I = 1 for winter and I = -1 for summer

ln is the natural logarithm.

In the link budget calculation, if G is the gain of the antenna (dB), the effective gain of the antenna equals G - ΔG_{BW}. For example, if a 20-degree antenna is used, the mean value of ΔG_{BW} would be close to 7 dB.

In [12], a very good agreement was found with the model presented above, based on extensive measurements in a flat suburban area with base station antenna height of 43 m and receive antenna heights of 5.2, 10.4 and 16.5 m, and 10^o receive antenna beamwidth. By comparing Figs. 5 and 6 in the paper, one can observe about 10 dB median GRF (difference between the directional and omnidirectional antenna median path loss) for the 5.2 m receive antenna height and distances 0.5-10 km. However, for the 10.4 and 16.5 receive antenna heights the difference (GRF) is smaller, about 7. More experimental data and analysis is desirable to describe more accurately the effects of different antenna heights and terrain types on the GRF values.

In system level simulations and link budget calculations for high cell coverage, the standard deviation of the GRF can also be accounted for. For a 20^o antenna, the standard deviation σ_{grf} is approximately 3 dB. Furthermore, we can expect that the variable component of the GRF is correlated with the shadow fading lognormal random variable (more scattering, i.e. larger GRF, when shadow fading is present). In [8], a clear trend for the GRF to increase as the excess path loss over free space path loss increases was shown (see also Fig. 5 below). The correlation coefficient between GRF and excess path loss about median path loss (equivalent to shadow fading loss) was found to be 0.77. No significant distance dependency of the median GRF was found. (The correlation coefficient between GRF and distance was found to be 0.12.)

The combined shadow fading/GRF standard deviation σ_c can be calculated using the following formula

$$\sigma_c^2 = \sigma^2 + \sigma_{grf}^2 + 2\rho\sigma\sigma_{grf}$$

where ρ is the correlation coefficient and σ is the standard deviation of the lognormal shadow fading random variable s. For σ = 8 dB and σ_{grf} = 3 dB the formula yields σ_c of 8.5 and 10.5 dB for ρ = 0 and ρ = 0.77, respectively. Larger standard deviation results in a larger path loss margin for the 90% cell coverage (approximately 0.3 dB for ρ = 0 and 1.5 dB for ρ = 0.77).

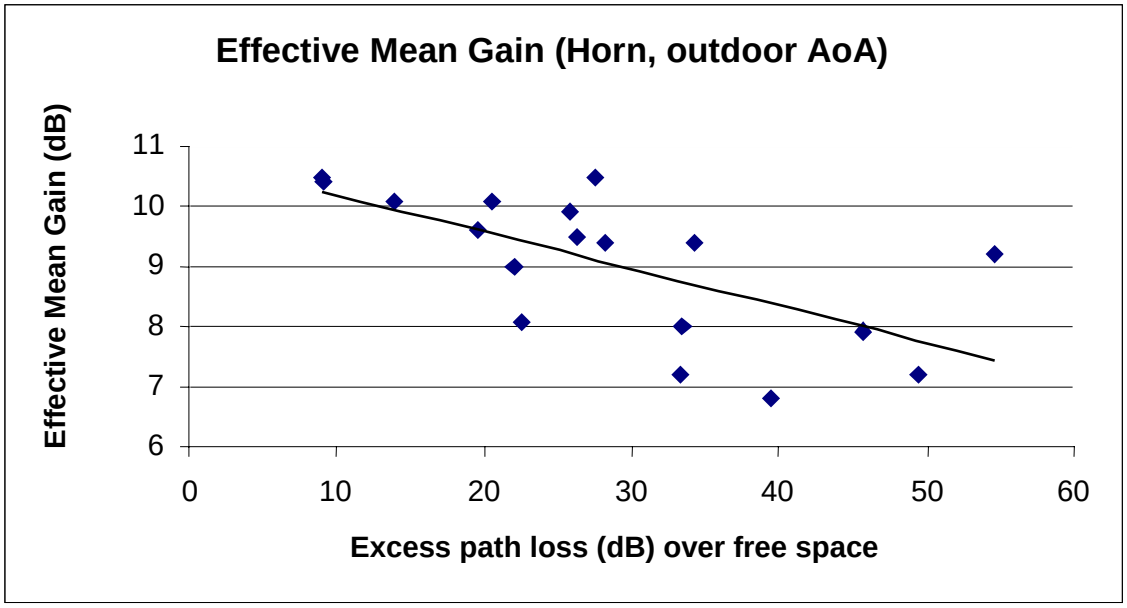

Figure 5. Effective mean (azimuth) gain for a 30-degree horn antenna.

For the results in Fig. 5, a BTS antenna height of 22 m was used, in a suburban area (Harlow, U.K.), in the summer. A 30° subscriber antenna was used, raised to gutter height as near as possible to houses being examined. The antenna was rotated in 15 degree steps, and the effective gain calculated from the maximum signal compared to the average signal (signals averaged through any temporal fading). The peak gain was 10.4 dB (this only accounts for azimuthal directivity).

Multiple Antenna Channel Models (MIMO)

When multiple antennas are used at the transmitter and/or at the receiver, the relationships between transmitter and receiver antennas add further dimensions to the model. The channel can be characterized by a matrix.

Modified Stanford University Interim (SUI) Channel Models

Channel models described above provide the basis for specifying channels for a given scenario. It is obvious that there are many possible combinations of parameters to obtain such channel descriptions. A set of 6 typical channels was selected for the three terrain types that are typical of the continental US [4]. In this section we present SUI channel models that we modified to account for 30^o directional antennas. These models can be used for simulations, design, development and testing of technologies suitable for fixed broadband wireless applications. The parameters were selected based upon statistical models described in previous sections.

The parametric view of the SUI channels is summarized in the following tables.

Terrain Type	SUI Channels
C	SUI-1, SUI-2
B	SUI-3, SUI-4
A	SUI-5, SUI-6

K-Factor: Low

Doppler	Low delay spread	Moderate delay spread	High delay spread
Low	SUI-3		SUI-5
High		SUI-4	SUI-6

K-Factor: High

Doppler	Low delay spread	Moderate delay spread	High delay spread
Low	SUI-1,2		
High			

The generic structure for the SUI Channel model is given below

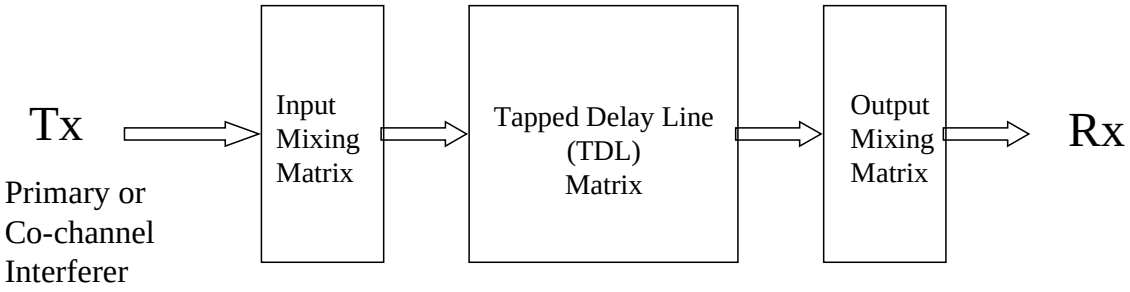

The above structure is general for Multiple Input Multiple Output (MIMO) channels and includes other configurations like Single Input Single Output (SISO) and Single Input Multiple Output (SIMO) as subsets. The SUI channel structure is the same for the primary and interfering signals.

Input Mixing Matrix: This part models correlation between input signals if multiple transmitting antennas are used.

Tapped Delay Line Matrix: This part models the multipath fading of the channel. The multipath fading is modeled as a tapped-delay line with 3 taps with non-uniform delays. The gain associated with each tap is characterized by a distribution (Ricean with a K-factor > 0, or Rayleigh with K-factor = 0) and the maximum Doppler frequency.

Output Mixing Matrix: This part models the correlation between output signals if multiple receiving antennas are used.

Using the above general structure of the SUI Channel and assuming the following scenario, six SUI channels are constructed which are representative of the real channels.

Scenario for modified SUI channels:

- Cell size: 7 km
- BTS antenna height: 30 m
- Receive antenna height: 6 m
- BTS antenna beamwidth: 120^{o}
- Receive Antenna Beamwidth: omnidirectional (360^{o}) and 30^{o}.
  For a 30^{o} antenna beamwidth, 2.3 times smaller RMS delay spread is used when compared to an omnidirectional antenna RMS delay spread [10]. Consequently, the 2^{nd} tap power is attenuated additional 6 dB and the 3^{rd} tap power is attenuated additional 12 dB (effect of antenna pattern, delays remain the same). For the omnidirectional receive antenna case, the tap delays and powers are consistent with the COST 207 delay profile models [18].
- Vertical Polarization only
- 90% cell coverage with 99.9% reliability at each location covered

For the above scenario, using the channel model, the following are the six specific SUI channels.

Notes:

1) The total channel gain is not normalized. Before using a SUI-X model, the specified normalization factors have to be added to each tap to arrive at 0dB total mean power (included in the tables).

2) The specified Doppler is the maximum frequency parameter (f_m) of the rounded spectrum, as described above.

3) The Gain Reduction Factor (GRF) is the total mean power reduction for a 30° antenna compared to an omni antenna. If 30° antennas are used the specified GRF should be added to the path loss. Note that this implies that all 3 taps are affected equally due to effects of local scattering.

4) K-factors have linear values, not dB values.

5) K-factors in the tables were rounded to the closest integer.

6) K-factors for the 90% and 75% cell coverage are shown in the tables, i.e. 90% and 75% of the cell locations have K-factors greater or equal to the K-factor value specified, respectively. For the SUI channels 5 and 6, 50% K-factor values are also shown.

SUI – 1 Channel				
	Tap 1	**Tap 2**	**Tap 3**	**Units**
Delay	0	0.4	0.9	μs
Power (omni ant.)	0	-15	-20	dB
90% K-fact. (omni)	4	0	0	
75% K-fact. (omni)	20	0	0	
Power (30° ant.)	0	-21	-32	dB
90% K-fact. (30°)	16	0	0	
75% K-fact. (30°)	72	0	0	
Doppler	0.4	0.3	0.5	Hz
Antenna Correlation: $\rho_{ENV} = 0.7$ **Gain Reduction Factor:** GRF = 0 dB **Normalization Factor:** F_{omni} = -0.1771 dB, $F_{30°}$ = -0.0371 dB			**Terrain Type:** C **Omni antenna:** $\tau_{RMS} = 0.111$ μs, overall K: K = 3.3 (90%); K = 10.4 (75%) **30° antenna:** $\tau_{RMS} = 0.042$ μs, overall K: K = 14.0 (90%); K = 44.2 (75%)	

SUI – 2 Channel

	Tap 1	Tap 2	Tap 3	Units
Delay	0	0.4	1.1	μs
Power (omni ant.)	0	-12	-15	dB
90% K-fact. (omni)	2	0	0	
75% K-fact. (omni)	11	0	0	
Power (30° ant.)	0	-18	-27	dB
90% K-fact. (30°)	8	0	0	
75% K-fact. (30°)	36	0	0	
Doppler	0.2	0.15	0.25	Hz

Antenna Correlation: $\rho_{ENV} = 0.5$
Gain Reduction Factor: GRF = 2 dB
Normalization Factor: $F_{omni} = -0.3930$ dB, $F_{30°} = -0.0768$ dB

Terrain Type: C
Omni antenna: $\tau_{RMS} = 0.202$ μs,
overall K: K = 1.6 (90%); K = 5.1 (75%)
30° antenna: $\tau_{RMS} = 0.069$ μs,
overall K: K = 6.9 (90%); K = 21.8 (75%)

SUI – 3 Channel

	Tap 1	Tap 2	Tap 3	Units
Delay	0	0.4	0.9	μs
Power (omni ant.)	0	-5	-10	dB
90% K-fact. (omni)	1	0	0	
75% K-fact. (omni)	7	0	0	
Power (30° ant.)	0	-11	-22	dB
90% K-fact. (30°)	3	0	0	
75% K-fact. (30°)	19	0	0	
Doppler	0.4	0.3	0.5	Hz

Antenna Correlation: $\rho_{ENV} = 0.4$
Gain Reduction Factor: GRF = 3 dB
Normalization Factor: $F_{omni} = -1.5113$ dB, $F_{30°} = -0.3573$ dB

Terrain Type: B
Omni antenna: $\tau_{RMS} = 0.264$ μs,
overall K: K = 0.5 (90%); K = 1.6 (75%)
30° antenna: $\tau_{RMS} = 0.123$ μs,
overall K: K = 2.2 (90%); K = 7.0 (75%)

SUI – 4 Channel

	Tap 1	Tap 2	Tap 3	Units
Delay	0	1.5	4	μs
Power (omni ant.)	0	-4	-8	dB
90% K-fact. (omni)	0	0	0	
75% K-fact. (omni)	1	0	0	
Power (30° ant.)	0	-10	-20	dB
90% K-fact. (30°)	1	0	0	
75% K-fact. (30°)	5	0	0	
Doppler	0.2	0.15	0.25	Hz

Antenna Correlation: $\rho_{ENV} = 0.3$
Gain Reduction Factor: GRF = 4 dB
Normalization Factor: $F_{omni} = -1.9218$ dB, $F_{30°} = -0.4532$ dB

Terrain Type: B
Omni antenna: $\tau_{RMS} = 1.257$ μs
overall K: K = 0.2 (90%); K = 0.6 (75%)
30° antenna: $\tau_{RMS} = 0.563$ μs
overall K: K = 1.0 (90%); K = 3.2 (75%)

SUI – 5 Channel

	Tap 1	Tap 2	Tap 3	Units
Delay	0	4	10	μs
Power (omni ant.)	0	-5	-10	dB
90% K-fact. (omni)	0	0	0	
75% K-fact. (omni)	0	0	0	
50% K-fact (omni)	2	0	0	
Power (30° ant.)	0	-11	-22	dB
90% K-fact. (30°)	0	0	0	
75% K-fact. (30°)	2	0	0	
50% K-fact. (30°)	7	0	0	
Doppler	2	1.5	2.5	Hz

Antenna Correlation: $\rho_{ENV} = 0.3$
Gain Reduction Factor: GRF = 4 dB
Normalization Factor: $F_{omni} = -1.5113$ dB, $F_{30°} = -0.3573$ dB

Terrain Type: A
Omni antenna: $\tau_{RMS} = 2.842$ μs
overall K: K = 0.1 (90%); K = 0.3 (75%); K = 1.0 (50%)
30° antenna: $\tau_{RMS} = 1.276$ μs
overall K: K = 0.4 (90%); K = 1.3 (75%); K = 4.2 (50%)

SUI – 6 Channel				
	Tap 1	**Tap 2**	**Tap 3**	**Units**
Delay	0	14	20	μs
Power (omni ant.)	0	-10	-14	dB
90% K-fact. (omni)	0	0	0	
75% K-fact. (omni)	0	0	0	
50% K-fact. (omni)	1	0	0	
Power (30° ant.)	0	-16	-26	dB
90% K-fact. (30°)	0	0	0	
75% K-fact. (30°)	2	0	0	
50% K-fact. (30°)	5	0	0	
Doppler	0.4	0.3	0.5	Hz

Antenna Correlation: $\rho_{ENV} = 0.3$
Gain Reduction Factor: GRF = 4 dB
Normalization Factor: $F_{omni} = -0.5683$ dB, $F_{30°} = -0.1184$ dB

Terrain Type: A
Omni antenna: $\tau_{RMS} = 5.240$ μs
overall K: K = 0.1 (90%); K = 0.3 (75%); K = 1.0 (50%)
30° antenna: $\tau_{RMS} = 2.370$ μs
overall K: K = 0.4 (90%); K = 1.3 (75%); K = 4.2 (50%)

.

Extension of Models to Other Frequencies

We expect that the proposed statistical models for delay spread, K-factor, and GRF can be “safely” used in the 1 – 4 GHz range (half and double frequency for which the models were derived). With appropriate frequency correction factors, path loss models can be also used in the extended frequency range [6]. However, the Doppler spectrum is a function of the center frequency and more work is required in this area.

Simulation

Appendix B describes how to simulate the SUI channel models based on a contribution by Stanford University.

Appendix A and Appendix B follow.

References

[1] Y. Okumura, E. Ohmori, T. Kawano, and K. Fukua, “Field strength and its variability in UHF and VHF land-mobile radio service,” *Rev. Elec. Commun. Lab*., vol. 16, no. 9, 1968.

[2] M. Hata, “Empirical formula for propagation loss in land mobile radio services,” *IEEE Trans. Veh. Technol*., vol. 29, pp. 317-325, Aug. 1980.

[3] EURO-COST-231 Revision 2, “Urban transmission loss models for mobile radio in the 900 and 1800 MHz bands,” Sept. 1991.

[4] V. Erceg et. al, “An empirically based path loss model for wireless channels in suburban environments,” *IEEE JSAC*, vol. 17, no. 7, July 1999, pp. 1205-1211.

[5] T.-S. Chu and L.J. Greenstein, “A quantification of link budget differences between the cellular and PCS bands,” *IEEE Trans. Veh. Technol.*, vol. 48, no. 1, January 1999, pp. 60-65.

[6] W.C. Jakes and D.O. Reudink, “Comparison of mobile radio transmission at UHF and X-band,” *IEEE Trans. Veh. Technol.*, vol. VT-16, pp. 10-13, Oct. 1967.

[7] K.V. S. Hari, K.P. Sheikh, and C. Bushue, “Interim channel models for G2 MMDS fixed wireless applications,” *IEEE 802.16.3c-00/49r2*

[8] M.S. Smith and C. Tappenden, “Additional enhancements to interim channel models for G2 MMDS fixed wireless applications,” *IEEE 802.16.3c-00/53*

[9] M.S. Smith, J.E.J. Dalley, “A new methodology for deriving path loss models from cellular drive test data”, *Proc. AP2000 Conference*, Davos, Switzerland, April 2000.

[10] V. Erceg et.al, “A model for the multipath delay profile of fixed wireless channels,” *IEEE JSAC*, vol. 17, no.3, March 1999, pp. 399-410.

[11] L.J. Greenstein, V. Erceg, Y.S. Yeh, and M.V. Clark, “A new path-gain/delay-spread propagation model for digital cellular channels,” *IEEE Trans. Veh. Technol.*, vol. 46, no. 2, May 1997.

[12] J.W. Porter and J.A. Thweatt, “Microwave propagation characteristics in the MMDS frequency band,” *ICC’2000 Conference Proceedings*, pp. 1578-1582.

[13] L.J. Greenstein, S. Ghassemzadeh, V.Erceg, and D.G. Michelson, “Ricean K-factors in narrowband fixed wireless channels: Theory, experiments, and statistical models,” *WPMC’99 Conference Proceedings*, Amsterdam, September 1999.

[14] D.S. Baum et.al., “Measurements and characterization of broadband MIMO fixed wireless channels at 2.5 GHz”, *Proceedings of ICPWC’2000*, Hyderabad, Dec. 2000.

[15] L. J. Greenstein and V. Erceg, “Gain reductions due to scatter on wireless paths with directional antennas,” *IEEE Communications Letters*, Vol. 3, No. 6, June 1999.

[16] V. Erceg, “Channel models for broadband fixed wireless systems,” *IEEE 802.16.3c-00/53*

[17] TAS 4500 RF Channel Emulator, Operations Manual

[18] "Digital Land Mobile Radio Communications - COST 207", Commission of the European Communities, Final Report, 14 March, 1984--13 September, 1988, Office for Official Publications of the European Communities, Luxembourg, 1989.

Appendix A

COST 231 WALFISCH-IKEGAMI MODEL

This model can be used for both urban and suburban environments. There are three terms which make up the model:

$$L_b = L_0 + L_{rts} + L_{msd}$$

L_0 = free space loss
L_{rts} = roof top to street diffraction
L_{msd} = multi - screen loss

free space loss :

$$L_0 = 32.4 + 20\log\left(\frac{R}{km}\right) + 20\log\left(\frac{f}{MHz}\right)$$

roof top to street diffraction

$$L_{rts} = -16.9 - 10\log\left(\frac{w}{m}\right) + 10\log\left(\frac{f}{MHz}\right) + 20\log\left(\frac{\Delta h_{mobile}}{m}\right) + L_{ori} \quad \text{for hroof} \rangle \text{hmobile}$$

$$= 0 \quad \text{for } L_{rts} < 0$$

where

$$L_{ori} = -10 + 0.354\frac{\varphi}{deg} \quad \text{for } 0 \le \varphi \le 35 \text{ deg}$$

$$= 2.5 + 0.075\left(\frac{\varphi}{deg} - 35\right) \quad \text{for } 35 \le \varphi \le 55 \text{ deg}$$

$$= 4.0 - 0.114\left(\frac{\varphi}{deg} - 55\right) \quad \text{for } 55 \le \varphi \le 90 \text{ deg}$$

and $\Delta h_{mobile} = h_{roof} - h_{mobile}$

The multi-screen diffraction loss

$$L_{msd} = L_{beh} + k_a + k_d \log\left(\frac{R}{km}\right) + k_f \log\left(\frac{f}{MHz}\right) - 9\log\left(\frac{b}{m}\right)$$

$= 0$ for $L_{msd} < 0$

$$L_{beh} = -18Log(1 + \frac{\Delta h_{base}}{m}) \quad \text{for } h_{base} \rangle h_{roof}$$

$= 0$ for $h_{base} \leq h_{roof}$

$k_a = 54$ for $h_{base} \rangle h_{roof}$

$= 54 - 0.8\frac{\Delta h_{base}}{m}$ for $R \geq 0.5$km and $h_{base} \leq h_{roof}$

$= 54 - 0.8\frac{\Delta h_{base}}{m}\frac{R/km}{0.5}$ for $R < 0.5$km and $h_{base} \leq h_{roof}$

$k_d = 18$ for $h_{base} \rangle h_{roof}$

$= 18 - 15\frac{\Delta h_{base}}{h_{roof}}$ for $h_{base} \leq h_{roof}$

$k_f = -4 + 0.7\left(\frac{f/MHz}{925} - 1\right)$ for medium sized cities and suburban centres with moderate tree density.

$= -4 + 1.5\left(\frac{f/MHz}{925} - 1\right)$ for metropolitan centres.

Note that $\Delta h_{base} = h_{base} - h_{roof}$

This model is limited by the following parameter ranges:

f : 800....2,000MHz,

h base : 4....50m,

h mobile: 1....3m

R : 0.02.....5km

Hata correction term in COST 231 W-I model to account for mobile height variation

Comparison with some measurements made by Nortel in 1996 for a base antenna deployed in Central London well above the average rooftop height revealed that the COST 231 W-I model did not correctly model the variation of path loss with mobile height. In contrast, the COST 231 Hata model did show the correct trend, which is not surprising, since it is an empirically derived model based on the very extensive measurement data of Okumura. Consequently, a Hata correction term has been added to the COST 231 W-I model to account for path loss variations with mobile height. However, the Hata correction term simply added to the COST 231 W-I model results in a path loss variation with mobile height that is greater than that of the Hata model. This is because it adds to the variation that exists already in the COST 231 W-I model. In the COST 231 W-I model the path loss variation due to mobile height is governed by the following term:

$$20\log\left(h_{roof} - h_{mobile}\right)$$

Here the Hata correction term is made to be zero at a mobile height of 3.5m. Retaining this, a new correction term is proposed as follows :

$$a(h_m) = -\left[\left(1.1\log\left(\frac{f}{MHz}\right) - 0.7\right)h_{mobile} - \left(1.56\log\left(\frac{f}{MHz}\right) - A\right) + 20\log\left(h_{roof} - h_{mobile}\right) - 20\log\left(h_{roof} - 3.5\right)\right]$$

where

$$A = 1.56\log\left(\frac{f}{MHz}\right) - \left(1.1\log\left(\frac{f}{MHz}\right) - 0.7\right)3.5$$

The term $a(h_m)$ is the correction factor and ensures that the COST 231 W-I model has the same path loss variation with mobile height as the COST 231 Hata model.

[END OF APPENDIX A]

Appendix B

[This information was originally submitted as Doc IEEE 802.16.3c-01/53]

Simulating the SUI Channel Models

Daniel S. Baum - Stanford University

The SUI Channel Models

This submission is an addendum to the contribution [EKSB01], which presents Channel Models for Fixed Wireless Applications and which contains the definition of a set of 6 specific channel implementations known as SUI channels. This paper is intended to help in the implementation of these models into a software channel simulator by elaborating on some issues that were not explained in detail and by providing Matlab[1] code that can act as a core for more extensive simulations.

Definitions

The parameters of the 6 SUI channels, including the propagation scenario that led to this specific set, are presented in the referenced document. As an example, the definition of the SUI-3 channel (older version) is reproduced below:

SUI – 3 Channel				
	Tap 1	**Tap 2**	**Tap 3**	**Units**
Delay	0	0.5	1	μs
Power (omni ant.)	0	-5	-10	dB
90% K Factor (omni ant.)	1	0	0	
Power (30^o ant.)	0	-11	-22	dB
90% K Factor (30^o ant.)	3	0	0	
Doppler	0.4	0.4	0.4	Hz
Antenna Correlation:	$\rho_{ENV} = 0.4$			
Gain Reduction Factor:	GRF = 3 dB			
Normalization Factor:	$F_{omni} = -1.5113$ dB, $F_{30°} = -0.3573$ dB			

Fig 1.) SUI-3 channel model definition

[1] MATLAB is a registered trademark of The Math Works, Inc.

The set of SUI channel models specify statistical parameters of microscopic effects (tapped delay line, fading, antenna directivity). To complete the channel model, these statistics have to be combined with macroscopic channel effects such as path loss and shadowing (also known as excess path loss) which are common to all 6 models in the set.

Each set model also defines an antenna correlation, which is discussed in more detail later in this document. The gain reduction factor (GRF) has also been included in the tables to indicate the connection with the K-factor.

Software Simulation

The aim of a software simulation can vary greatly, the range spans from statistical analysis to communication signal simulations. The approach to coding for a task can therefore differ significantly depending on the goal. For the purpose of demonstrating the model implementation, we concentrate on the core channel simulation, i.e. the result of our code is to produce channel coefficients at an arbitrary (channel) sampling rate.

Power Distribution

We use the method of filtered noise to generate channel coefficients with the specified distribution and spectral power density. For each tap a set of complex zero-mean Gaussian distributed numbers is generated with a variance of 0.5 for the real and imaginary part, so that the total average power of this distribution is 1. This yields a normalized Rayleigh distribution (equivalent to Rice with K=0) for the magnitude of the complex coefficients. If a Ricean distribution (K>0 implied) is needed, a constant path component *m* has to be added to the Rayleigh set of coefficients. The ratio of powers between this constant part and the Rayleigh (variable) part is specified by the K-factor. For this general case, we show how to distribute the power correctly by first stating the total power P of each tap:

$$P = |m|^2 + \sigma^2, \qquad (2.1)$$

where m is the complex constant and σ^2 the variance of the complex Gaussian set. Second, the ratio of powers is

$$K = \frac{|m|^2}{\sigma^2}. \qquad (2.2)$$

From these equations, we can find the power of the complex Gaussian and the power of the constant part as

$$\sigma^2 = P\frac{1}{K+1} \text{ and } |m|^2 = P\frac{K}{K+1}. \qquad (2.3a/b)$$

From eqns. 2.3 we can see that for K=0 the variance becomes P and the constant part power diminishes, as expected. Note that we choose a phase angle of 0° for m in the implementation.

Doppler Spectrum

The random components of the coefficients generated in the previous paragraph have a white spectrum since they are independent of each other (the autocorrelation function is a Dirac impulse). The SUI channel model defines a specific power spectral density (PSD) function for these scatter component channel coefficients called ‘rounded’ PSD which is given as

$$S(f) = \begin{cases} 1 - 1.72 f_0^2 + 0.785 f_0^4 & |f_0| \le 1 \\ 0 & |f_0| > 1 \end{cases} \quad \text{where} \quad f_0 = \frac{f}{f_m}. \tag{2.4}$$

To arrive at a set of channel coefficients with this PSD function, we correlate the original coefficients with a filter which amplitude frequency response is derived from eqn. 2.4. as

$$|H(f)| = \sqrt{S(f)}. \tag{2.5}$$

We choose to use a non-recursive filter and the frequency-domain overlap-add method for efficient implementation. We also have to choose some filter length which determines how exact and smooth our transfer function is realized by the filter.

Since there are no frequency components higher than f_m, the channel can be represented with a minimum sampling frequency of 2 f_m, according to the Nyquist theorem. We therefore simply define that our coefficients are sampled at a frequency of 2 f_m.

The total power of the filter has to be normalized to one, so that the total power of the signal is not changed by it. The mean energy of a discrete-time process $x(k)$ is

$$E\left\{|x(k)|^2\right\} = \frac{1}{N}\sum_{k=1}^{N}|x(k)|^2 = \int_{-\pi}^{\pi} S_{xx}(e^{j\Omega})\, d\Omega, \text{ where } \Omega = 2\pi f / f_s. \tag{2.6}$$

We note that the PSD function given in eqn. 2.4 is not normalized.

Antenna Correlation

The SUI channel models define an antenna correlation, which has to be considered if multiple transmit or receive elements, i.e. multiple channels, are being simulated. Antenna correlation is commonly defined as the envelope correlation coefficient between signals received at two antenna elements. The received baseband signals are modeled as two complex random processes $X(t)$ and $Y(t)$ with an envelope correlation coefficient of

$$\rho_{env} = \left| \frac{E\{(X - E\{X\})(Y - E\{Y\})^*\}}{\sqrt{E\{|X - E\{X\}|^2\}E\{|Y - E\{Y\}|^2\}}} \right|. \tag{2.7}$$

Note that this is not equal to the correlation coefficient of the envelopes (magnitude) of two signals, a measure that is also used frequently in cases where no complex data is available.

Since the envelope correlation coefficient is independent of the mean, only the random parts of the channel are of interest. In the following we therefore consider the random channel components only, to simplify the notation.

In the general case of frequency selective (delay-spread) propagation, the channel is modeled as a tapped-delay line:

$$g(t,\tau) = \sum_{l=1}^{L} g_l(t)\delta(\tau - \tau_l) \tag{2.8}$$

where L is the number of taps, $g_l(t)$ are the time-varying tap coefficients and τ_l are the tap delays.

We now calculate the correlation coefficient between two receive signals $r_1(t)$ and $r_2(t)$, which are the result of a normalized, random, white transmitted signal $s(t)$ propagating through two channels with the channel impulse responses $g_1(t,\tau)$ and $g_2(t,\tau)$:

$$g_i(t,\tau) = \sum_{l=1}^{3} g_{il}(t)\delta(\tau - \tau_l),\ i \in [1..2] \tag{2.9}$$

Note that in the SUI channel models the number of taps is L=3 and that the tap delays τ_l are fixed (independent of i). Assuming that equivalent taps in both channels have equal power:

$$\sigma_{1l}^2 = \sigma_{2l}^2 = \sigma_l^2,\ l \in [1..3] \tag{2.10}$$

and that taps with different delays are uncorrelated within a channel as well as between channels:

$$E\left\{g_{ik}(t)g_{jl}^*(t)\right\} = 0,\ \forall k \neq l \text{ where } k,l \in [1..3];\ i,j \in [1..2] \tag{2.11}$$

the antenna correlation coefficient becomes:

$$\rho_{env} = \left| \frac{\rho_1\sigma_1^2 + \rho_2\sigma_2^2 + \rho_3\sigma_3^2}{\sigma_1^2 + \sigma_2^2 + \sigma_3^2} \right| \tag{2.12}$$

where ρ_l are the correlation coefficients between each of the 3 pairs of taps $g_{1l}(t)$ and $g_{2l}(t)$:

$$\rho_l = \frac{E\left\{g_{1l}(t)g_{2l}^*(t)\right\}}{\sigma_{1l}^2\sigma_{2l}^2},\ l \in [1..3] \tag{2.13}$$

From eqn. 2.12 we can see how the antenna correlation can be related to the individual tap correlations, where σ_l^2 are the individual tap gains. To obtain a simple solution for setting these tap correlations depending on the required antenna

correlation, we can additionally demand all tap correlations to be equal. Then eqn. 2.12 simply states that all tap correlations have to be set to the antenna correlation. For the simulation of the SUI channel we recommend setting all tap correlations equal to the antenna correlation.

To generate a sequence of random state vectors with specified first order statistics (mean vector μ and correlation matrix R), we can use the following transformation [MiEG99]:

$$\tilde{V} = R^{1/2} V + \mu , \tag{2.14}$$

where V is a vector of independent sequences of Gaussian-distributed random numbers with zero mean and identical variance. The correlation matrix R is defined and factored as:

$$R = E\left\{ \begin{bmatrix} 1 & r_{12} & \cdots \\ r_{12}^{*} & 1 & \cdots \\ \vdots & \vdots & \ddots \end{bmatrix} \right\} = R^{1/2} R^{H/2} , \tag{2.15}$$

If we use eqn. 2.14 to correlate complex sequences, not all correlations between real and imaginary parts of the input sequences are set according to the specified envelope correlation coefficient. To correlate complex sequences, we therefore split each complex sequence into real and imaginary part and correlate the real-valued sequences. For example, to correlate two complex sequences X and Y, the input vector V and the correlation matrix R are set as:

$$V = \begin{bmatrix} \mathrm{Re}\{X\} \\ \mathrm{Im}\{X\} \\ \mathrm{Re}\{Y\} \\ \mathrm{Im}\{Y\} \end{bmatrix}, \; R = \begin{bmatrix} 1 & 0 & \rho_{env} & \rho_{env} \\ 0 & 1 & \rho_{env} & \rho_{env} \\ \rho_{env} & \rho_{env} & 1 & 0 \\ \rho_{env} & \rho_{env} & 0 & 1 \end{bmatrix} \tag{2.16}$$

To implement correlated channels in our simulation, first two independent but equally distributed set of channel coefficients are created following the procedures given in the beginning of chapter 2. Then we use eqns. 2.14 and 2.16 to correlate the random signals of equivalent taps in these two channels.

In a general vector or matrix channel, correlation coefficients can be defined between all sub-channels.

Observation Rate

For some purposes it can be required or useful to have the SUI channel coefficients at an arbitrary chosen observation rate, i.e. the data rate of a communication system. This can be done easily by resampling the channel data to the specific sampling rate.

Matlab Coding

Matlab Coding

Based on the discussion in the previous chapter, the coding in Matlab is straightforward. In the following we will demonstrate this by an example implementation of the SUI-3 omni antenna channel. Apart from the basic simulation processing we also provide code to generate supplementary results which might be of interest and can help to improve understanding. This additional code is displayed in gray outlined boxes titled 'Additional Info'.

Let us first define the simulation parameters

`N = 10000;`	number of independent random realizations
`OR = 4;`	observation rate in Hz
`M = 256;`	number of taps of the Doppler filter
`Dop_res = 0.1;`	Doppler resolution of SUI parameter in Hz (used in resampling-process)
`res_accu = 20;`	accuracy of resampling process

and the SUI channel parameters (SUI-3/omni used here):

`P = [ 0 -5 -10 ];`	power in each tap in dB
`K = [ 1 0 0 ];`	Ricean K-factor in linear scale
`tau = [ 0.0 0.5 1.0 ];`	tap delay in µs
`Dop = [ 0.4 0.4 0.4 ];`	Doppler maximal frequency parameter in Hz
`ant_corr = 0.4;`	antenna correlation (envelope correlation coefficient)
`Fnorm = -1.5113;`	gain normalization factor in dB

First we calculate the power in the constant and random components of the Rice distribution for each tap:

```
P       = 10.^(P/10);                          % calculate linear power
s2      = P./(K+1);                            % calculate variance
m2      = P.*(K./(K+1));                       % calculate constant power
m       = sqrt(m2);                            % calculate constant part
```

Additional Info: RMS delay spread

```
rmsdel  = sqrt( sum(P.*(tau.^2))/sum(P) - (sum(P.*tau)/sum(P))^2 );
fprintf('rms delay spread  %6.3f µs\n', rmsdel);
```

Now we can create the Ricean channel coefficients with the specified powers.

```
L       = length(P);                           % number of taps
paths_r = sqrt(1/2)*(randn(L,N) + j*randn(L,N)).*((sqrt(s2))' * ones(1,N));
paths_c = m' * ones(1,N);
```

Before combining the coefficient sets, the white spectrum is shaped according to the Doppler PSD function. Since the frequency-domain filtering function `FFTFILT` expects time-domain filter coefficients, we have to calculate these first. The filter is then normalized in time-domain.

```
for p = 1:L
   D     = Dop(p) / max(Dop) / 2;              % normalize to highest Doppler
   f0    = [0:M*D]/(M*D);                      % frequency vector
   PSD   = 0.785*f0.^4 - 1.72*f0.^2 + 1.0;     % PSD approximation
   filt  = [ PSD(1:end-1) zeros(1,M-2*M*D) PSD(end:-1:2) ]; % S(f)
   filt  = sqrt(filt);                         % from S(f) to |H(f)|
   filt  = ifftshift(ifft(filt));              % get impulse response
   filt  = real(filt);                         % want a real-valued filter
   filt  = filt / sqrt(sum(filt.^2));          % normalize filter
   path  = fftfilt(filt, [ paths_r(p,:) zeros(1,M) ]);
   paths_r(p,:) = path(1+M/2:end-M/2);
end;
paths   = paths_r + paths_c;
```

Now that the fading channel is fully generated, we have to apply the normalization factor and, if applicable, the gain reduction factor

```
paths   = paths * 10^(Fnorm/20);               % multiply all coefficients with F
```

Additional Info: average total tap power

```
Pest = mean(abs(paths).^2, 2);
fprintf('tap mean power level: %0.2f dB\n', 10*log10(Pest));
```

Additional Info: spectral power distribution

```
figure, psd(paths(1,:), 512, max(Dop));
```

In a multichannel scenario, the taps between different channels have to be correlated according to the specified antenna correlation coefficient. Assuming that two random channels have been generated `in paths1 = paths_r1 + paths_c1` and `paths2 = paths_r2 + paths_c2` following the procedures above, we can now apply the correlation

```
rho  = ant_corr;                               % desired correlation is ant_corr
R  = sqrtm([  1   0  rho rho ; ...             % factored correlation matrix
              0   1  rho rho ; ...
             rho rho  1   0  ; ...
             rho rho  0   1  ]);
V  = zeros(4,L,N);
V(1,:,:) = real( paths_r1 );                   % split complex coefficients
V(2,:,:) = imag( paths_r1 );
V(3,:,:) = real( paths_r2 );
V(4,:,:) = imag( paths_r2 );
for l = 1:L
   V(:,l,:) = R*squeeze(V(:,l,:));             % transformation
end;
paths_r1 = squeeze(V(1,:,:)) + j*squeeze(V(2,:,:));   % combine complex coefficients
```

```
paths_r2 = squeeze(V(3,:,:)) + j*squeeze(V(4,:,:));

paths1 = paths_r1 + paths_c1;                    % add mean/constant part
paths2 = paths_r2 + paths_c2;
```

Additional Info: estimate envelope correlation coefficient

```
disp('estimated envelope correlation coefficients between all taps in both paths');
disp('matrix rows/columns: path1: tap1, tap2, tap3, path2: tap1, tap2, tap3');
abs(corrcoef([ paths1; paths2]'));
```

Finally, we resample the current rate to the specified observation rate. In order to use the Matlab polyphase implementation `resample`, we need the resampling factor F specified as a fraction $F = P/Q$.

```
SR = max(Dop)*2;                                 % implicit sample rate
m  = lcm(SR/Dop_res, OR/Dop_res);
P  = m/SR*Dop_res;                               % find nominator
Q  = m/OR*Dop_res;                               % find denominator
paths_OR = zeros(L,ceil(N*P/Q));                 % create new array
for p=1:L
   paths_OR(p,:) = resample(paths(p,:), P, Q, res_accu);
end;
```

The resampled set of channel coefficients for all the 3 taps are now contained in the matrix `paths_OR`. The total simulated observation period of the channel is now $SR \cdot N = OR \cdot \text{ceil}(N \cdot P/Q)$, where $SR = 2 \cdot \max(Dop)$.

Some Exemplary Results

Now that we have implemented a core simulator for the SUI channels, we will use it to generate some plots about the statistical characteristics of these channels. All simulations use the settings as defined above (SUI-3/omni), if not otherwise stated.

To get a first impression, fig. 2 shows a signal magnitude plot of the channel coefficients over time.

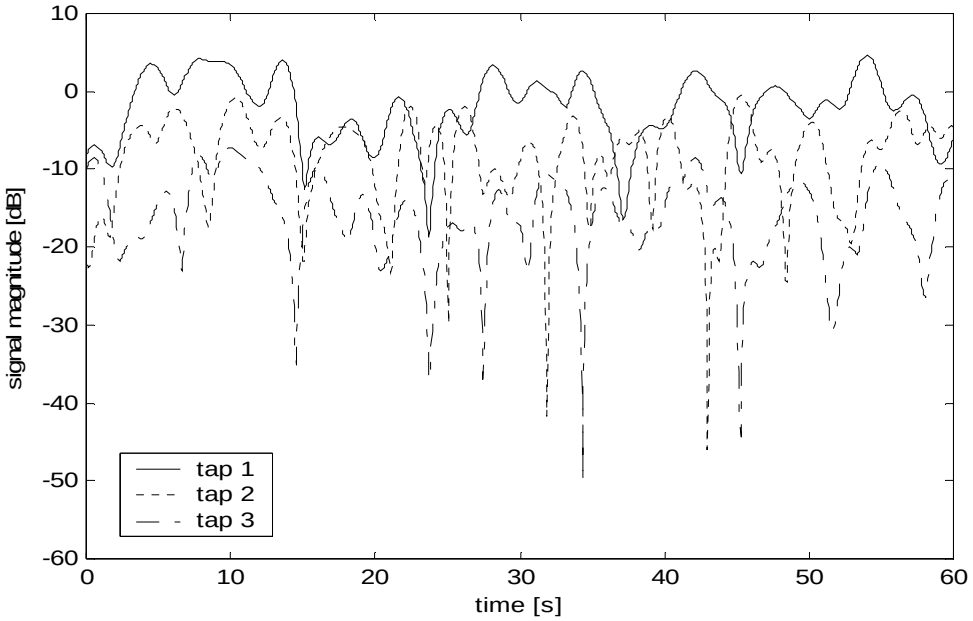

Fig 2.) Fading Plot (OR=20Hz)

For statistical purposes, the observation rate is of no significance to the result as long as it is higher than the original sampling rate. However, increasing the observation rate can sometimes help to smoothen distribution functions.

Fading Distributions

The distribution of power levels at the output of a channel is one of the important properties of a channel. Depending on the assumed input signal spectral power distribution, we can define 3 basic cases for the 'channel power':

narrowband signal: PSD: $S(f) = \delta(f_C)$

flat bandpass signal: PSD: $S(f) = 1/BW \cdot rect_{BW}(f - f_C)$

flat wideband signal: PSD: $S(f) = \lim_{BW \to \infty} \left[1/BW \cdot rect_{BW}(f - f_C)\right]$

The higher the bandwidth of a channel, the less likely a deep fade occurs for the total channel power (frequency diversity effect). Fig. 3 illustrates this effect by showing the probability of the signal magnitude falling below a certain level. Note that channel power distributions are generally not Ricean, except for the narrowband case.

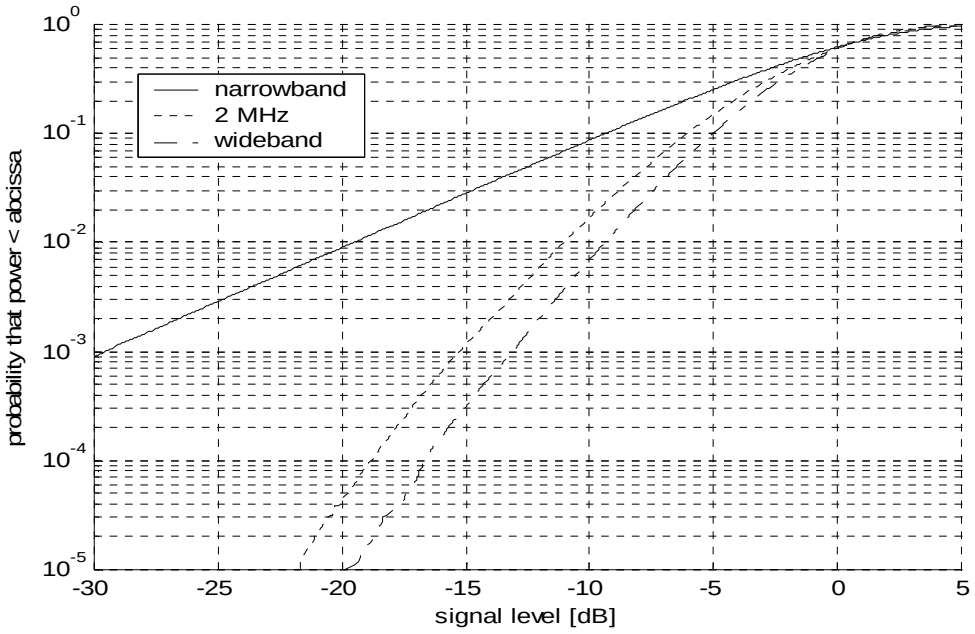

Fig 3.) CDF of channel power (N=200000, OR=4Hz)

Level Crossing Rates / Average Duration of Fades

The level crossing rate (LCR) and average duration of fade (ADF) functions are commonly used for examining the combined effect of fade distribution and Doppler spectrum. The LCR function shows the rate of the signal magnitude dropping below a certain level and the ADF function shows the average duration below that level. These graphs can be useful for choosing and evaluating channel codes for this particular channel.

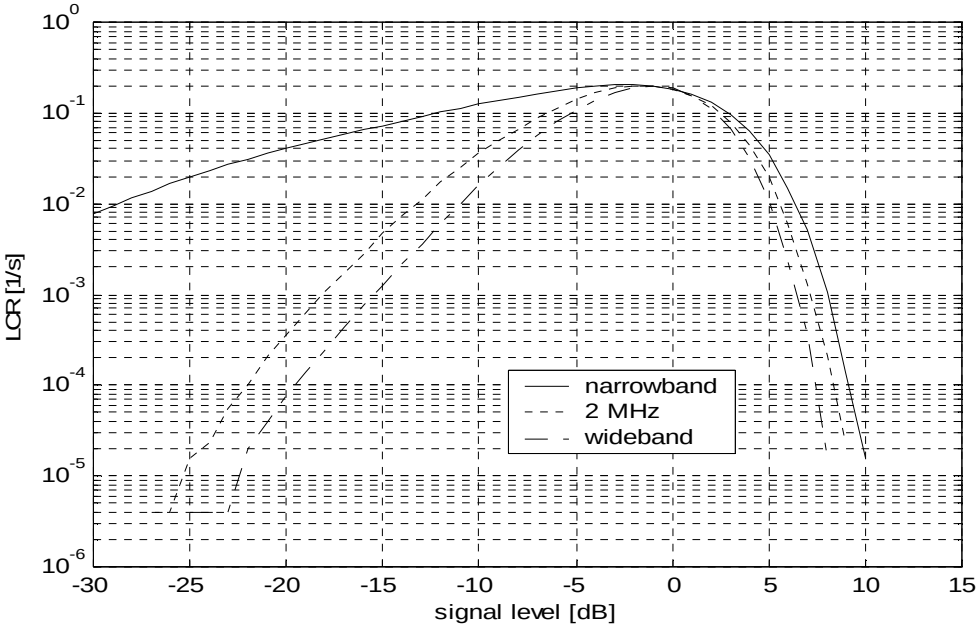

Fig 4.) LCR (N=200000, OR=10Hz)

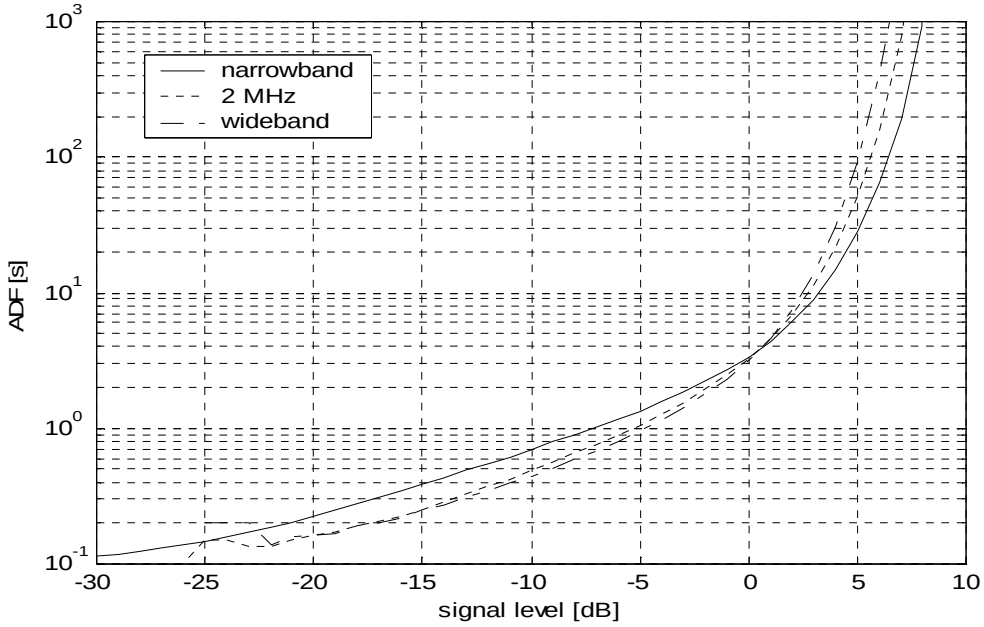

Fig 5.) ADF (N=200000, OR=10Hz)

References

[EKSB01] V. Erceg, K.V.S. Hari, M.S. Smith, D.S. Baum et al, “Channel Models for Fixed Wireless Applications”, IEEE 802.16.3 Task Group Contributions 2001, Feb. 01

[MiEG99] D.G. Michelson, V. Erceg and L.J. Greenstein, “Modeling Diversity Reception Over Narrowband Fixed Wireless Channels”, in *MTT-S Symp. on Tech. for Wireless Applic.*, 1999, pp. 95-100

[END OF APPENDIX B]